Analyst

Accepted Manuscript

ROYAL SOCIETY OF CHEMISTRY

www.rsc.org/analyst

Analyst

RSCPublishing

COMMUNICATION

On-Chip Dilution in Nanoliter Droplets

Cite this: DOI: 10.1039/xoxxoooooox

Raviraj Thakur[a], Ahmed M. Amin[b] and Steve Wereley[a]

Received ooth January 2012,
Accepted ooth January 2012

DOI: 10.1039/xoxxoooooox

www.rsc.org/

Droplet microfluidics is enabling reactions at nano- and picoliter scale, resulting in faster and cheaper biological and chemical analyses. However, varying concentrations of samples on a drop-to-drop basis is still a challenging task in droplet microfluidics, primarily limited due to lack of control over individual droplets. In this paper, we report an on-chip microfluidic droplet dilution strategy using three-valve peristaltic pumps.

Concentration screens are central to most biological/chemical assays in drug discovery. They reveal key quantitative information about the dynamics of assay components. Mainstream examples include the evaluation of Michaelis rate constant (K_m) for enzyme-substrate kinetics, determining half-maximal inhibitory concentration of a drug (IC50) by constructing dose-response data and estimating association/dissociation constants (K_d) of protein complexes from binding affinities measurement. These parametric studies are also important for optimization assays such as co-crystal and protein crystallization screens for generating concentration-dependent phase diagrams.

Consequently, dilution is a fundamental step in concentration screens. Manual pipetting of samples and mixing with dilution buffers in various ratios is a time consuming task. Robotic liquid handlers are capable of alleviating this issue by performing automated serial dilutions; however, they are expensive and generally consume sample volumes in the microliter range. Lab-on-chip devices are particularly promising with respect to lower sample consumption and process automation. Several microfluidic dilution schemes exist and can be broadly classified into two main fields: pneumatic on-chip valve-based and droplet-based systems.

Urbanski et al.[1] pioneered a cascaded dilution scheme using a ring mixer. In their device, sample and buffer were mixed in 1:1 ratio to generate 2 fold dilution in one step. Higher order dilutions were achieved by serially combining the mixed product again with the buffer. Although the process was completely automated, the dilution ratio per step is invariant and is imposed by the channel geometry. Moreover, the process is time consuming for dilutions of higher orders, as it requires several intermediate metering, mixing and temporary storage steps. Paegel et al.[2] modified the concept by employing a single intermediate storage reservoir. However, their approach was susceptible to cross contamination from intermediate runs. Microfluidic serial dilution networks[3,4] have been reported that utilize diffusion-based mixing in microchannels to generate samples with different concentrations. In such devices, sample and dilution buffer are mixed using a T/Y-junction and the resultant dilution ratios depend on hydraulic channel resistances and flow rate parameters. Ismagilov et al.[5] first used this continuous-flow approach as the input to a droplet generation channel. The flow rate ratio of sample to diluent was varied to obtain a different concentration in resulting droplets. Similar techniques with a split-and-combine approach were used with more complex networks that emulsified droplets[6,7] with wider concentration range. These methods suffer from fixed dilution ratios which cannot be actively controlled due to predetermined channel geometry.

[a] Birck Nanotechnoloy Center, School of Mechanical Engineering, Purdue University, West Lafayette, IN 47907, USA.
[b] Microfluidic Innovations, West Lafayette, IN 47907, USA.
†Electronic Supplementary Information (ESI) available: Workflow of droplet dilution using 3-valve on-chip pumps.

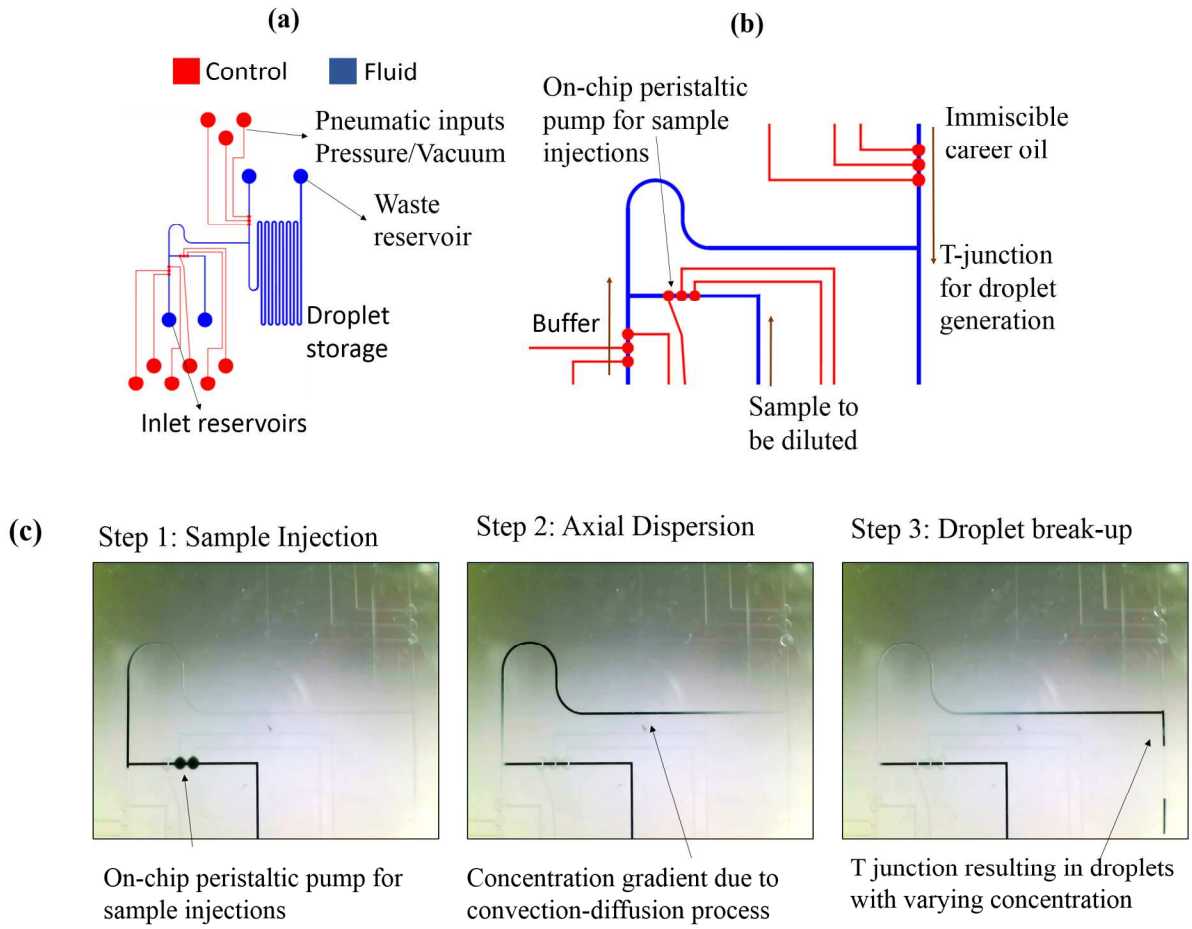

Figure 1: (a) Microfluidic chip layout showing liquid (blue) and control layer (red) channels. I/O ports for pipetting fluids and pneumatic signals as well as droplet storage area are shown. (b) Close-up view showing 3-valve peristaltic pumps for the dilution buffer, sample to be diluted and the carrier oil phase. (c) Droplet dilution workflow. In the first step, the peristaltic pump is used to inject sample into an injection zone. In the second step, the buffer stream is advanced towards a T junction. Axial concentration gradient develops because of convection-diffusion of the sample. This gradient plug is digitized into droplets with varying concentration in the final step.

Recently, a direct droplet dilution scheme was developed by Niu et al.[8] where a parent droplet having a high concentration was trapped in a microchannel using hydrodynamic resistance and back pressure due to surface tension. Droplets of dilution buffer were coalesced into it and split in sequence to achieve a 4-order concentration gradient over 30 droplets. However, trapping the parent droplet required some optimal flow rate conditions. Different reagents viscosities, interfacial tensions (and thus hydrodynamic resistance) lead to different trapping conditions. To address these issues, stagnation regions were used to firmly trap parent droplets, and the dilution buffer stream was passed through to induce partial diffusion-based mixing leading to a streamwise gradient[9,10]. The stream was then segmented using an immiscible oil phase through a traditional T-junction to generate varying concentration droplets. However, the trapped droplets in the stagnation zones are potentially difficult to remove for successive runs and require flow rate modulation of higher orders. Moreover, in both the above methods, external pumping was required to generate droplets which complicates chip-to-world interfacing.

Recently, Cai etal.[11] used of axial dispersion of solute to create concentration gradients in droplets to perform biochemical screening of enzyme inhibitors. This method was then utilized by Miller etal.[12] to perform large scale screening of drug compound library. However, both methodologies lacked a programmable control over dilution range, which is a desired feature for any screening application. Also, use of external pumps permitted droplets to stay inside chips for <3.5 minutes. This method can be challenging to adopt for studying slower kinetics especially in cell based screening or crystallization applications. In this communication, we present a dilution protocol by using a programmable microfluidic component: a three-valve peristaltic pump, to vary concentration from drop-to-drop. Briefly, a high concentration sample is injected using these on-chip pumps into a steady stream of buffer. The buffer with the sample pulse and an immiscible oil phase are co-flowed through a T-junction in an alternating manner to produce a series of nanoliter droplets. As

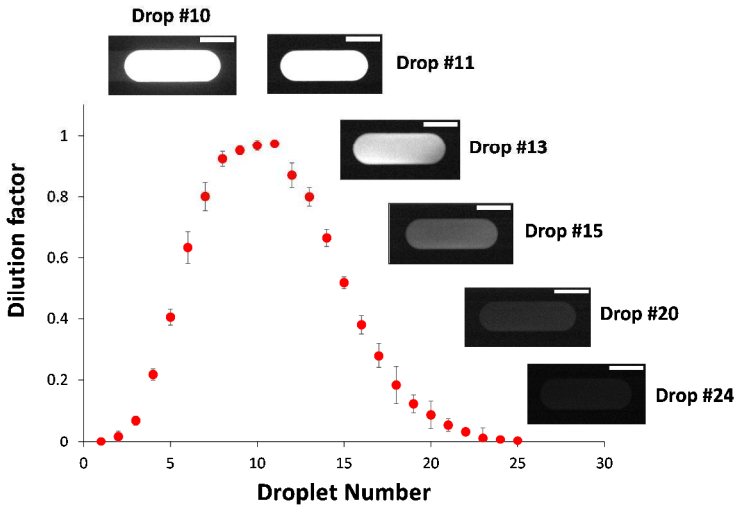

General Pseudo Code

Initialize:

Pump 1 for sample; Pump 2 for diluent buffer, Pump 3 for FC3283 oil

1) Set the number of Pump 1 units = X
// (Injected sample volume)
2) Set the number of droplets before next injection = Y
// determine the range of dilution
3) Set the number of repetitions= Z

Execute:
Loop Z times **//(replicates of a sequence)**
{
Pump *Pump 1* X units
// inject sample to be diluted
Loop Y times **// No. of droplets before next injection.**
{
Pump *Pump 2* 1 unit **// Droplet production**
Pump *Pump 3* 1 unit **// using alternate pumping**
}
}

Figure 2 *(left)* Concentration gradient in successive droplets. Four pump cycles of CF488 fluorescent dye was used during the injection stage. Concentration gradient can be clearly seen with variable greyscale intensity levels of the inset droplet images. The scale bar in each photograph is equivalent to 100µm. (*right*) a general pseudo code demonstrating the workflow in droplet dilution sequence.

the sample pulse advances, the combined effect of diffusion and convection produces a concentration gradient in the streamwise direction resulting in a droplet sequence with varying concentration. Furthermore, we demonstrate that by programming the number of droplets produced after sample injection step, dilution range of a sequence can be modulated. For preliminary demonstrations, three droplet sequences were created with 3 fold, 80 fold and 6000 fold dilution. Drop-on demand enables generation of small number of droplets which can be docked inside the chips till the completion of assay. Such programmable control is a highly desired feature for broad range of biological screening applications.

The microfluidic chip was assembled from three separately made layers, a liquid layer, a gas control layer and a flexible membrane. The fluid and the control layers were fabricated using an inverse replica molding of poly-dimethylsiloxane (PDMS, 184 Sylguard) with a negative tone SU8-3050 (MicroChem) photoresist. The PDMS polymer and curing agent were mixed in a 10:1 ratio by weight, poured over the SU8 masters and baked at 75^0C for 5 hrs. The channel depths were 40µm for both layers. Part of the PDMS mixture was spin coated on a glass slide at 1300 rpm for 1300 sec to obtain a thin flexible PDMS membrane. The membrane was plasma bonded to the control layer and aligned with the liquid layer to obtain a three layer assembly.

The schematic of the device is shown in fig 1(a, b). Three inlet reservoirs were designed for pipetting 10µL aliquot of dilution buffer (DI water), 0.5µL aliquot of a high concentration sample (food colour dyes/CF488) and 10µL aliquot of an immiscible oil phase (fluorocarbon oil FC3283, 3M Corp.) respectively. On-chip peristaltic pumps were used to drive all fluids as opposed to external syringe pumps, which are typically used in droplet microfluidics. The pumps consisted of three normally closed valves[13] placed in series, each of which was forced open/close by applying vacuum/pressure over the flexible membrane layer through control channel lines. Peristaltic flow was generated by actuating the valves in a 5-phase sequence. The rate of valve actuation was controlled using a software-programmable microvalve controller unit[14] (Microfluidic Innovations, Indiana). For the current study, the pump period was kept constant at 2 sec.

Fig 1(c) shows three principle steps of the microfluidic droplet dilution workflow: 1) sample injection, 2) axial dispersion, and 3) programmable droplet generation. Initially, dilution buffer is used to prime the microchannels until the end of the injection zone. The droplet generation channel is primed with a fluorocarbon oil (FC3283). A program is written that encodes the pump states for each of the three pumps for the entire droplet dilution workflow. An example of a high level pseudo code is provided in Fig 2(right). During the first step, a finite sample volume was injected into the injection zone by controlling the number of pump cycles. For the purposes of Fig 2(left), 4 pump cycles were used to inject a highly concentrated CF488 fluorescent dye into the static buffer. The sample pulse maintains a sharp profile, since it is primarily subjected to dispersion due to molecular diffusion in the static buffer. In the second step, the peristaltic pump driving the dilution buffer is used to advance this sample plug towards a T-junction (100µm × 40µm). An axial concentration gradient is set up in the buffer stream owing to the convection-diffusion process. As a final step, the concentration gradient plug is converted into droplets of approximately 5.2nL volume with a generation frequency of 0.25Hz. For highly consistent droplet volumes, the buffer pump and the oil pump pulsed fluids in an alternate manner into the T-junction. The droplet dilution can be clearly seen in fig 2(left) where the grayscale intensity varies as a function of droplet number.

The dilution process was quantified using CF488 dye (0.1mM) to estimate the concentration in each droplet resulting from the

combined effect of convection-diffusion under the pulsed flow conditions. A CCD camera (PCO1600) was used to capture intensity signals sufficiently downstream of the droplet generation junction in order to ensure homogeneous concentration in every droplet. First, reference measurements were made with droplets of DI water, oil stream, and a parent sample with known concentration of CF488 (0.1mM in DI water). The illumination intensity and the initial dye concentration were chosen such that it nearly saturated CCD camera. This allowed maximum utilization of the dynamic range of CCD, thus enabling measurements of dilution range up to 100 fold. Next, a dilution program was run to obtain droplet train with varying concentrations. The background greyscale intensity level was subtracted from the obtained signal, and the outcomes were normalized against the known sample intensities to obtain a dilution factor. Fig 2(left) shows the variation of dilution factor as a function of droplet number.

To further quantify this dilution strategy, we characterized the effect of initial sample volume and number of droplets generated on the resulting concentration gradient profile. The droplet sizes were kept constant around 5.2nL using single alternating pump strokes as previous experiment. During the first step of sample injection, the concentration profile is nearly rectangular in shape. As this rectangular pulse of sample traverses downstream under the influence of peristaltic pumps, the peak height of the concentration profile attenuates; while the pulse width undergoes broadening effect due to combined effect of advection-diffusion. Hence, the location of T junction for droplet generation and initial sample volume plays a crucial role in determining the peak height of dilution factor profile. It is imperative to have at least one droplet in the dilution sequence with concentration identical to the initial sample concentration from inlet reservoir. The location of T junction from the point of injection is dictated by geometrical design and cannot be changed dynamically. Thus, we investigated the effect of sample volume on the peak height of the dilution factor curve, for the same T junction downstream location. We created droplet sequences with different initial sample volumes by changing the number of pump strokes during sample injection step. A program was written to execute four replicate droplet sequences for each sample volume. The resulting droplet dilution factors of the sequence can be seen in figure 3 (top). Each pulse in the plot represents a droplet from the dilution sequence. In accordance with the advection-diffusion theory, a general characteristic trend was observed with peak

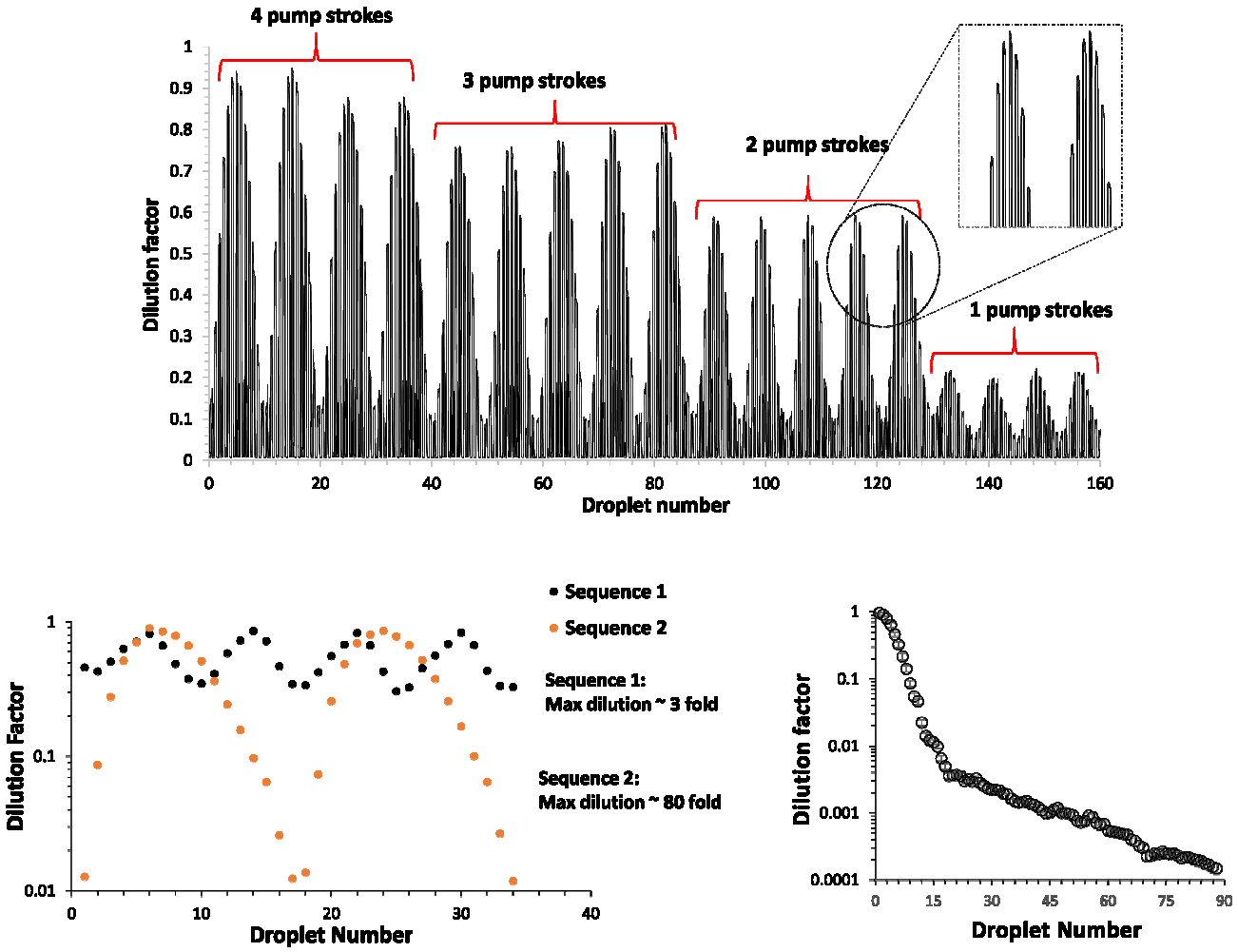

Figure 3 (*top*) Effect of sample volume on the dilution factor range. It can be seen that with decreasing initial sample volumes, the peak of the dilution factor decreases due to combined effect of convection-diffusion. A minimal of 4 pump stroke equivalent volume is need during the sample injection step. (*bottom left*) Droplet sequences with tunable dilution range. Two droplet sequences are generated having 3 fold and 80 fold dilution range. By controlling the number of droplets generated after sample injection, the dilution degree can be modulated. (*bottom right*) A sequence of 90 droplets yields a dilution of ~6000 fold.

height of the dilution curve decreasing with decreasing sample volume. A sample volume equivalent to 4 pump strokes resulted in a droplet array with peak height of 0.95, while a sample volume equivalent to 1 pump strokes resulted in the peak height of 0.2. Based on these experimental observations, we conclude that minimal of 4 pump stroke equivalent sample volume is needed to obtain the peak height of dilution curve close to unity. The loss of 5% in the concentration is attributed to initial mixing of the sample with the residual diluent buffer.

The dilution factor range can be further modified effectively by controlling the number of droplets produced at T junction after the sample injection step. Figure 3 (bottom left) shows two droplet sequences, each having same initial sample volume (4 pump strokes), while the number of droplets produced between successive sample injections are 10 and 18 respectively. It can be clearly seen that the dilution range is different for these sequences. The sequence of 10 droplets after sample injection produced droplet dilution sequence up to ~3 fold, while sequence of 18 droplets resulted in dilution by ~80 fold. Our programmable microvalve controller unit allows users to set arbitrary values for number of pump strokes for sample injection, number of droplets generated per injection and replicates of each sample before the start of each experiment (Fig 2 right). Thus, there is no restriction to the number of droplets generated in a particular sequence per sample injection. To validate this hypothesis, we have measured a dilution of ~6000 fold by increasing the number of droplets to 90 as depicted in Figure 3 (bottom right).

The dilution scheme presented here has many advantages over existing methods. It uniquely combines the software programmable, valve-based lab-on-chip technology with the two phase droplet microfluidics approach to vary concentration from drop-to-drop. On-chip peristaltic pumping permits on-demand generation of droplets without requiring any auxiliary external fluid pumping components, thereby simplifying world-to-chip interfacing. Sample/reagents can be pipetted using an HPLC autosampler directly into the reservoirs without appreciable dead volumes. The droplets can be stopped on-demand in the channels for detection, allowing both kinetic and equilibrium measurements to yield high quality information. From fig 3(*bottom right*), it can be seen that the concentration is spread across almost 3 orders within 90 droplets. Each droplet represents a data point with specific conditions, hence multiple droplets will lead to high density and statistically high confidence data. The inherent programmability of the peristaltic pumps mean that scripts with arbitrary set of instructions can be executed to yield highly complicated droplet patterns, which are otherwise difficult to generate with external pumping mechanisms. We demonstrated that the dilution range can be modulated in two ways. First, the amount of sample injected can be controlled by varying the number of pump strokes. Second, the dilution range can be increased by increasing the number of droplets generated between successive sample injections. For the current study, the droplet volumes were one pump stroke equivalent, however larger droplets can be generated on-demand by controlling the number of pump strokes during droplet formation process. This feature can enable *coarse to fine screening* strategy and will be tested in the future work. For example, a user can select a custom dilution range with a coarse gradient using large droplet volumes or a high definition gradient with least droplet volumes. Moreover, axial dispersion in low Reynolds number flows is a well-studied phenomenon. For a flow in a convection dominated regime, the concentration gradient becomes independent of molecular diffusion constant of input sample. Thus, we can built calibration curves to predetermine the concentration in each droplet, and how it varies as a function of sample volume, number of droplets and droplet size. An example of such theoretical calibration function can be found in electronic supplementary material (section 2).

All biochemical samples such as proteins/DNAs/small molecules etc. are precious, as they are extracted with extensive time and cost consuming processes. A microfluidic platform that can obtain high definition and large amount of information from smallest sample volumes will be of immense use. As a next step towards building a complete screening platform, we will develop and integrate droplet merging and mixing module into the current device. The platform will be used for studying model systems such as enzyme-inhibition assays for building high quality dose-response data and protein-protein interactions.

References:

1. J. P. Urbanski, W. Thies, C. Rhodes, S. Amarasinghe, and T. Thorsen, *Lab Chip*, 2006, **6**, 96–104.
2. B. M. Paegel, W. H. Grover, A. M. Skelley, R. a Mathies, and G. F. Joyce, *Anal. Chem.*, 2006, **78**, 7522–7.
3. K. Lee, C. Kim, B. Ahn, R. Panchapakesan, A. R. Full, L. Nordee, J. Y. Kang, and K. W. Oh, *Lab Chip*, 2009, **9**, 709–17.
4. C. Kim, K. Lee, J. H. Kim, K. S. Shin, K.-J. Lee, T. S. Kim, and J. Y. Kang, *Lab Chip*, 2008, **8**, 473–9.
5. H. Song and R. F. Ismagilov, *J. Am. Chem. Soc.*, 2003, **125**, 14613–9.
6. C.-G. Yang, Z.-R. Xu, A. P. Lee, and J.-H. Wang, *Lab Chip*, 2013, **13**, 2815–20.
7. M. N. Bui, C. A. Li, K. N. Han, J. Choo, E. K. Lee, and G. H. Seong, *Anal. Chem.*, 2011, 1603–1608.
8. X. Niu, F. Gielen, J. B. Edel, and A. J. deMello, *Nat. Chem.*, 2011, **3**, 437–42.
9. M. Sun, S. S. Bithi, and S. a Vanapalli, *Lab Chip*, 2011, **11**, 3949–52.
10. M. Sun and S. a Vanapalli, *Anal. Chem.*, 2013, **85**, 2044–8.
11. L.-F. Cai, Y. Zhu, G.-S. Du, and Q. Fang, *Anal. Chem.*, 2012, **84**, 446–52.
12. O. Miller and A. El Harrak, *Proc. Natl. Acad. Sci.*, 2012, **109**, 1–6.
13. W. H. Grover, R. H. C. Ivester, E. C. Jensen, and R. a Mathies, *Lab Chip*, 2006, **6**, 623–31.
14. A. M. Amin, R. Thakur, S. Madren, H.-S. Chuang, M. Thottethodi, T. N. Vijaykumar, S. T. Wereley, and S. C. Jacobson, *Microfluid. Nanofluidics*, 2013, **15**, 647–659.